
Mixing Configurations for Downstream Prediction

Anonymous Author(s)

Affiliation
Address
email

Abstract

1 Humans possess an innate ability to group objects by similarity—a cognitive mechanism
2 that clustering algorithms aim to emulate. Recent advances in community
3 detection have enabled the discovery of *configurations*—valid hierarchical clusterings
4 across multiple resolution scales—without requiring labeled data. In this
5 paper, we formally characterize these configurations and identify similar emergent
6 structures in register tokens within Vision Transformers. Unlike register tokens,
7 configurations exhibit lower redundancy and eliminate the need for ad hoc se-
8 lection. They can be learned through unsupervised or self-supervised methods,
9 yet their selection or composition remains specific to the downstream task and
10 input. Building on these insights, we introduce GraMixC, a plug-and-play mod-
11 ule that extracts configurations, aligns them using our novel Reverse Merge/Split
12 (RMS) technique, and fuses them via attention heads before forwarding them to
13 any downstream predictor. On the DSNI 16S rRNA cultivation-media prediction
14 task, GraMixC improves the R^2 from 0.6 to 0.9 on various methods, setting a new
15 state-of-the-art. We further validate GraMixC across standard tabular benchmarks,
16 where it consistently outperforms single-resolution and static-feature baselines.

1 Introduction

18 Learning general-purpose features that enhance down-
19 stream tasks has been a long-standing goal in machine
20 learning. One prominent example is clustering (*i.e.*, com-
21 munity detection) in unsupervised learning, which aims
22 to group entities so that objects in the same cluster are
23 similar, while objects in different clusters are dissimi-
24 lar, without relying on any labels [1]–[3]. Interestingly,
25 this paradigm demonstrates remarkable similarities to
26 human-like behaviors. Decades of cognitive science
27 studies show that even infants have the ability to group
28 objects by similarity [4], [5]. In particular, they often
29 organize them at different abstraction levels [6], [7]. In-
30 spired by this, recent advances in community detection
31 have extended clustering to the discovery of *configura-*
32 *tions*—hierarchical clusterings that span multiple reso-
33 lution scales [8]. For example, as illustrated in Fig. 1, in-
34 *lin-eage diagram* in Fig. 1, in the CIFAR10 dataset [9],
35 coarse configurations may separate vehicles from ani-
36 mals, while finer configurations distinguish between
37 birds, cats, and dogs. These multi-resolution representa-
38 tions reveal rich hierarchical structures that could pro-
vide stronger priors or inductive biases for deep models. However, despite their potential,

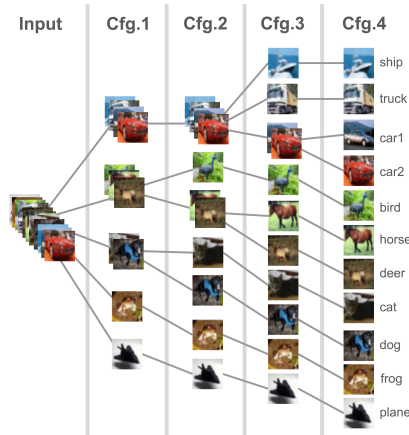


Figure 1: Illustration of CIFAR10 configura-
tions. Each column represents clustering
at a specific resolution—a configura-

39 such configurations remain largely underexplored in deep learning, especially in challenging domains
40 where labels are sparse.

41 One such domain is 16S ribosomal RNA (rRNA) gene sequencing, a widely used tool in microbiome
42 studies for identifying and classifying bacteria. Analyzing 16S rRNA data has consistently confronted
43 significant challenges in downstream prediction tasks within label-scarce environments. Previous
44 works in 16S rRNA representation learning have demonstrated substantial benefits for bacterial
45 taxonomic profiling and microbial community analysis [10]–[12]. Notably, Johnson et al. [13]
46 showed that full-length sequencing combined with appropriate clustering of intragenomic sequence
47 variation can provide more accurate representation of bacterial species in microbiome datasets. These
48 findings underscore the importance of learning clustered representations without relying on labels.

49 Recent methodologies typically transform clustering results into pseudo-labels to enhance down-
50 stream prediction performance. For instance, DeepCluster [14] iteratively clusters CNN-extracted
51 visual features and leverages these cluster assignments to guide network parameter updates. Graph-
52 based methods such as [15] employ structural clustering to overcome limitations of traditional
53 contrastive learning approaches that depend on positive and negative sample pairs. Their method
54 captures structural relationships among nodes in heterogeneous information networks, establishing a
55 self-supervised pre-training framework that learns robust network representations from unlabeled
56 data. Nevertheless, aforementioned approaches predominantly focus on a single configuration type,
57 overlooking the potential benefits of mixing configurations across multiple resolution scales.

58 In this paper, we introduce GraMixC, a plug-and-play module that extracts, aligns and mixes graph-
59 based configurations for downstream prediction. The main contributions of the paper are as follows:

- 60 • We identify three key characteristics of clustering configurations through systematic exper-
61 imental analysis, providing a novel perspective on enhancing downstream prediction via
62 mixing configurations.
- 63 • We propose GraMixC, a plug-and-play module based on mixed configurations. We apply it
64 to a novel 16S rRNA cultivation-media prediction task, setting a new state-of-the-art.
- 65 • We further conduct extensive experiments on multiple standard tabular benchmarks to
66 validate GraMixC’s effectiveness, where it consistently outperforms single-resolution and
67 static-feature baselines.

68 The remainder of this paper is organized as follows. Section 2 analyzes behavioral patterns of
69 configurations. Section 3 details our proposed GraMixC. Section 4 evaluates GraMixC’s performance
70 through extensive experiments. Finally, Section 5 concludes the paper. Our data and implementation
71 is available at <https://anonymous.4open.science/r/project-34CB>.

72 2 Preliminary results

73 We first present preliminary experimental results on configurations using CIFAR10. Specifically,
74 we compare patterns of configurations with those of the learnable “register” tokens in a recent
75 vision transformer DINoV2-reg [16]. Fig. 2 shows the attention maps from our configurations and
76 their register tokens. Moreover, Fig. 3 shows qualitative behaviors of our configurations and their
77 quantitative advantages over registers in terms of feature importance and neighborhood similarity.
78 From these results, we identify three key properties:

79 **Configurations emerge via unsupervised or self-supervised learning.** We define Near ground truth
80 (GT) balls as balls selected with the highest clustering scores, marked yellow in Fig. 2a. As shown in
81 Fig. 2b, the attention map, acquired by feeding configurations as tokens to attention heads for linear
82 probing, yields high norm regions substantially overlap with GT balls. On another hand, DINoV2-reg
83 exhibits similar attention map patterns in selected registers (see Fig. 2c), which might be related to
84 registers activating different areas in Fig. 2d, similar to slot attention [16]–[19]. Thus, based on the
85 similar attention map behavior, register token can be considered as a latent configuration.

86 **Configurations are selected and mixed based on input and task.** *Configuration selection and*
87 *mixing* refers to learning which resolution scales to focus on for a given downstream task. We
88 visualize this via attention maps over configuration tokens, where high-norm regions indicate the
89 selected scales. In Fig. 2b, attention norms vary across rows, showing that each input sample triggers
90 different resolution scales. Without any change to the configurations, we merge the original labels

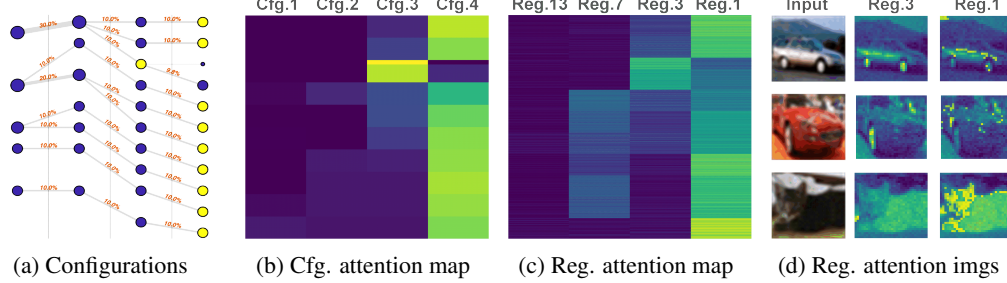


Figure 2: Comparison of attention maps obtained from configurations and registers, rows for samples. **(a)**: Lineage diagram for configurations, near GT balls are marked yellow. **(b)**: Attention map of configuration tokens in an attention-based linear probing. **(c)**: Attention map of DINOv2-reg register tokens, mean of all patch norms is used. **(d)**: Attention maps over the register tokens, as images.

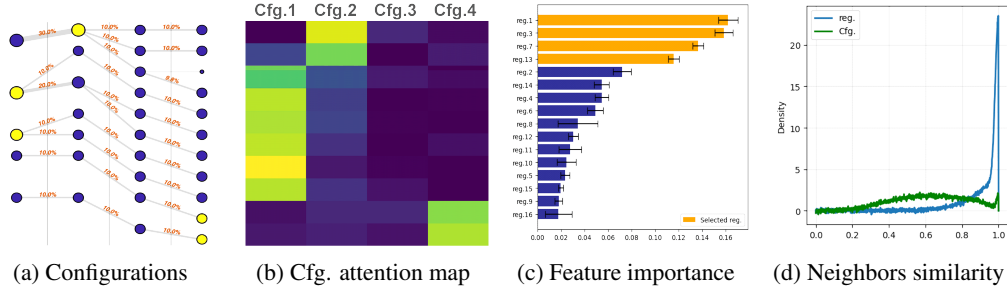


Figure 3: Illustration of another two properties of configurations, grouped by left two and right two. **(a)**: Lineage diagram where coarser classes are used for GT. **(b)**: Attention map in linear probing the coarser classes. **(c)**: Distribution of feature vector importance over the register tokens querying, mean of all patch importance is used. **(d)**: Distribution of cosine similarity between query embeddings of register and configuration tokens and their 2 neighbors, mean of all patch similarities is used.

91 into coarser classes (Fig. 3a) and plot the new attention map (Fig. 3b). The attention shifts to align
 92 with the coarser GT, whereas DINOv2-reg register tokens remain unchanged unless re-trained. These
 93 observations confirm that configuration selection and mixing are input- and task-dependent.

94 **Configurations are more informative and less redundant than register tokens.** Register tokens
 95 can help extract configurations, similar to object detection [20], [21], but selecting a fixed number by
 96 feature importance is arbitrary and non-rigorous (see Fig. 3c). Furthermore, register tokens exhibit
 97 high redundancy—cosine similarity between their embeddings and their 2 neighbors embeddings is
 98 heavily skewed toward 1—whereas configurations yield information less redundant (see Fig. 3d).

99 3 Methodology

100 Having these characterizations, we hypothesize that unsupervised methods can produce hierarchical
 101 *multi-resolution clusterings*, and that task- and input-specific *selection and mixing* of these configura-
 102 tions represent *global information* beneficial to downstream tasks. Building on the hypothesis, we
 103 propose a lightweight module *GraMixC*, that treats configurations as tokens ([CFG]) and incorporates
 104 a novel alignment layer plus learnable attention heads [22] after the configuration extraction model,
 105 enabling task- and input-specific mixing of configurations via end-to-end back-propagation.

106 Fig. 4 illustrates *GraMixC*. Given an input matrix $\mathbf{X} \in \mathbb{R}^{N \times d}$ (with N samples and feature dimen-
 107 sion d), *GraMixC* pass \mathbf{X} to two branches: (1) a path to unsupervised learning box that extracts
 108 configurations, and (2) a direct path to the downstream predictor. If at inference, we apply *Reverse*
 109 *Merge & Split* (RMS) alignment on the configurations. Then we pass them to positional encoding (PE)
 110 and attention heads. The final concatenation is passed to a downstream predictor for the prediction \hat{y} .

111 Except for the downstream predictor, the *GraMixC* model can be divided into three parts: the
 112 unsupervised learning of configurations, the Reverse Merge & Split (RMS) for alignment, and

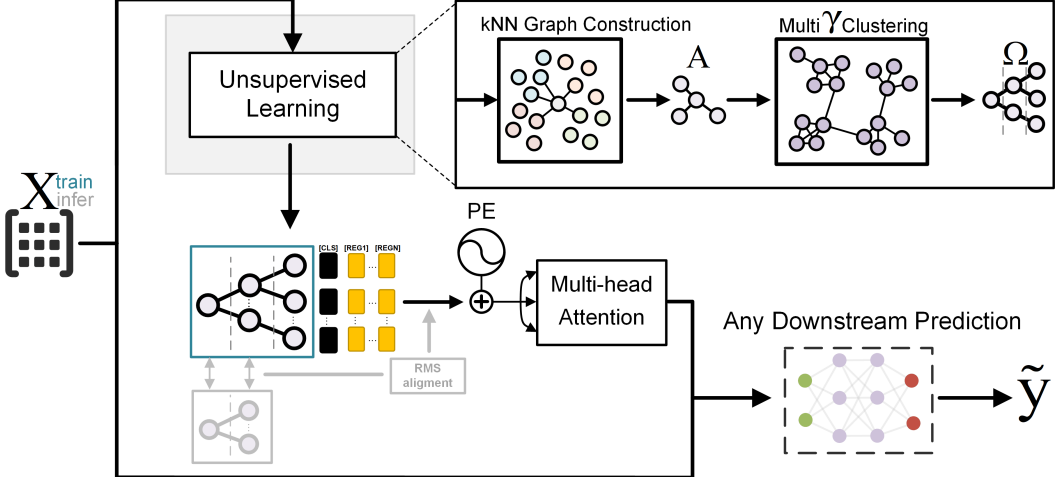


Figure 4: Illustration of the proposed GraMixC module and resulting model. The input data branches into (upper) a path to unsupervised learning box that extracts configurations, and (lower) a direct path to the downstream predictor. Their outcomes concatenate and pass to the downstream predictor. The components occur only during training and inference are colored in blue and gray, respectively.

113 attention heads for fusion. In the attention heads part, following Dariset et al. [16], we append register
 114 tokens ([REG]) after [CFG] and [CLS] for a clean attention map, that can be used backwards to guide
 115 configuration selection . Below we detail the rest two components in Section 3.1 and Section 3.2.

116 3.1 Multi-resolution graph-based clustering

117 Given \mathbf{X} , multi-resolution clustering seeks to extract *configurations*—valid hierarchical clusterings
 118 across multiple resolution scales—which we denote as $\Omega \in \mathbb{N}^{N \times m}$, where m denotes the number of
 119 valid resolution levels. To preserve the latent manifold structure in data, ease parameter sensitivity, and
 120 prevent other problems with traditional clustering methods (see Appendix B), we choose the resolution
 121 parameter ($\gamma \in \mathbb{R}_+$)-based community detection as our core clustering method. While BlueRed [23]
 122 can conduct graph clustering without problems like resolution limit or parameter sensitivity in
 123 traditional methods, recent work by Pitsianis et al. [8] further demonstrates the elimination of γ
 124 selection, and enabled the unsupervised discovery of Ω and the corresponding set of all valid γ , which
 125 is denoted as $\Gamma = \{\gamma_1^*, \gamma_2^*, \dots, \gamma_m^*\} \subseteq [0, \infty)$. Inspired by these works, the unsupervised box in
 126 Fig. 4 unfolds into two steps: **(1) k-nearest neighbors (kNN) [24] graph construction**, which return
 127 a directed graph $G = (V, E)$, usually represented as adjacency matrix $\mathbf{A} \in \mathbb{R}_+^{N \times N}$, and **(2) multi- γ**
 128 **clustering** on the resulted graph, i.e. modularity based community detection with unsupervised Γ
 129 learning, which return the wanted Ω . The details for each of these two steps are:

130 **(1) kNN graph construction.** We construct a kNN graph with $k = \log_{10} N$ as convention, using
 131 Euclidean distance for simplicity. Such pair-wise geometric distance between two different vertexes
 132 is denoted $d(\mathbf{x}_i, \mathbf{x}_j)$ where $i \neq j$ and $\mathbf{x}_i \in \mathbb{R}^d$ is the i -th feature vector. We then have the adjacency
 133 matrix \mathbf{A} formulated as: $A_{ij} = d(\mathbf{x}_i, \mathbf{x}_j)$ if $(\mathbf{x}_i, \mathbf{x}_j) \in E$, 0 otherwise, where E is the edge set
 134 of the kNN graph and A_{ij} denotes the i -th row and j -th column element of the adjacency matrix.
 135 Then we force *column stochastic* by dividing each column in the constructed \mathbf{A} with the column
 136 sum. The resulted graph is sparse stochastic, and we can apply Stochastic Graph t-SNE (SG-t-SNE)
 137 reweighting [25], which proved to remedy skewed degree distribution, that is not promised by
 138 conventional t-SNE [26]. From the original work, the key equations for SG-t-SNE reweighting are:

$$w(\mathbf{x}_i, \mathbf{x}_j) = \frac{1}{\lambda} \exp \left(-\frac{d^2(\mathbf{x}_i, \mathbf{x}_j)}{2\sigma_i^2} \right), \quad \text{with} \quad \lambda = \sum_{\mathbf{x}_j: (\mathbf{x}_i, \mathbf{x}_j) \in E} \exp \left(-\frac{d^2(\mathbf{x}_i, \mathbf{x}_j)}{2\sigma_i^2} \right),$$

139 where λ is a non-negative parameter constant, which we simply set to 15 as previous work show
 140 that it is not so sensitive to the choice of λ [25], and σ_i is a variable to be numerically solved with
 141 bisection method. After giving value of w to d , we have \mathbf{A} with less skewed degree distribution,
 142 which avoids problems like numerical instability and bias towards hubs in downstream clustering.

143 **(2) multi- γ community detection.** Then one may simply pass the reweighted \mathbf{A} to γ -based com-
 144 munity detection method, such as Leiden algorithm [27], to get one pseudo-configuration vector
 145 $\omega_\gamma \in \{1, \dots, N\}^N$ (“pseudo” for not sure to be valid). However, such γ falls in the range of $[0, \infty)$,
 146 and searching over all possible γ is exhausting. Therefore, we incorporate the BlueRed method with
 147 parallel descending triangulation (parallel-DT) [8], in order to automatically discover all valid $\gamma^* \in \Gamma$.
 148 Given a fixed γ , BlueRed find the optimal configuration ω_γ by the following optimization:

$$\omega_\gamma = \arg \min_{\omega \in \{1, \dots, N\}^N} \left[- \sum_{k=1}^{|\omega|_\infty} \sum_{(i,j) \in E} d(\mathbf{x}_i, \mathbf{x}_j) \mathbf{1}_{\omega_i = \omega_j = k} + \gamma \sum_{k=1}^{|\omega|_\infty} \sum_{(i,j) \in E} d^2(\mathbf{x}_i, \mathbf{x}_j) \mathbf{1}_{\omega_i = k}, \right],$$

149 where ω_i denotes the i -th element of ω , $|\omega|_\infty = \max_{i \leq N} \omega_i$ is a inf-norm, and $\mathbf{1}$ denotes the indicator
 150 gate which take value 1 if its subscript condition holds, 0 otherwise. Pitsianis et al. [8] describe the
 151 first term as attraction and the second term as repulsion. Optimizing each solely yields all-in-one
 152 configuration $\omega_0 = [1, 1, \dots, 1]$ and all-lonely configuration $\omega_\infty = [1, 2, \dots, N]$. Between these
 153 two configurations, parallel-DT allows forming BlueRed Front (BRF) [8] by segmenting $(0, \infty)$ into
 154 m ranges, among which each has a dominant γ_i^* yields lower HAR [8]—the sum of first term and the
 155 negative second term—which means “local minimum” on that range. Thus desired Ω is formed.

156 3.2 RMS: reverse merge & split alignment

157 Multi-resolution clustering on different datasets $\mathbf{X}_{\text{train}}$ and \mathbf{X}_{test} often naturally produces misaligned
 158 configurations, that either (1) have different value of m or $|\omega|_\infty$, or (2) have different cluster labels.
 159 While (2) is not a problem as re-assigning fix it, (1) could be problematic as the length and position
 160 of configurations influence the downstream fusion. One possible interpretation is that some clusters
 161 are further merged or split in another configuration, leading to this mismatch. To address this, we
 162 propose Reverse Merge & Split (RMS), which identifies an optimal alignment, allowing re-merging
 163 and re-splitting, between two configurations, ω_i and ω_j . First of all, an alignment score is defined:

$$\text{SCORE}(\omega_i, \omega_j) = \text{ARI}(\omega_i, \omega_j) - \theta \left| \frac{|\omega_i|_\infty - |\omega_j|_\infty}{|\omega_i|_\infty + |\omega_j|_\infty} \right|.$$

164 where θ is a hyperparameter to balance the weights of the two terms, which we set to 0.1, ARI is the
 165 adjusted rand index as defined in Hubert and Arabie [28]. By this punished ARI design, we consider
 166 different labels, merge and split during scoring the alignment between two partition, but also avoids
 167 too much difference in number of clusters (one extreme case is ω_0 and ω_∞ has ARI of 1).

168 However, the SCORE itself does not convey the mapping we need for reassigning. In RMS alignment,
 169 we construct a confusion matrix $\mathbf{C} \in \mathbb{N}^{|\omega_i|_\infty \times |\omega_j|_\infty}$ between ω_i and ω_j . As an assignment problem
 170 with a rectangle cost matrix $-\mathbf{C}$, it is solvable by twisting existing Hungarian algorithm methods [29]–
 171 [31]. Because \mathbf{C} is the adjacency matrix of a bipartite graph, spectral reordering via its graph
 172 Laplacian is preferred, since it encodes global connectivity and reveals coherent split–merge structures
 173 rather than merely optimizing diagonal entries. As the Fiedler vector reordering [32] assumes
 174 symmetric positive semi-definite, it is not directly applicable to \mathbf{C} . Inspired by a recent work of
 175 Floros, Pitsianis, and Sun [33], we introduce a two-walk Laplacian, which is defined as:

$$\mathbf{L}_{\text{tw}} = \mathbf{D} - \mathbf{C}_{\text{tw}}, \quad \text{with } \mathbf{C}_{\text{tw}} = \begin{bmatrix} \mathbf{C}\mathbf{C}^\top & \mathbf{C} \\ \mathbf{C}^\top & \mathbf{C}^\top\mathbf{C} \end{bmatrix},$$

176 where $\mathbf{D} = \text{diag}(\mathbf{C}_{\text{tw}}\mathbf{1})$ is the diagonal degree matrix of \mathbf{C}_{tw} . We remap ω_i and ω_j by using,
 177 respectively, the first $\|\omega_i\|_\infty$ and the last $\|\omega_j\|_\infty$ entries in the Fiedler eigenvector of \mathbf{L}_{tw} , which
 178 is the eigenvector corresponds to smallest positive eigenvalue. We further reverse split and merge
 179 simply by reassigning the redundant columns or rows who has element larger than its diagonal entry.

180 In GraMixC, we carry a small portion (0.1%) of train samples as *anchors* during inference, and the
 181 portion of Ω_{train} and Ω_{test} corresponding to the anchors are used to calculate the SCORE. Given m is
 182 usually small, we exhaustively test pairs (ω_i, ω_j) then iteratively pick the pair yielding the highest
 183 SCORE for each ω_i . For each pair, we apply the mapping from $\text{RMS}(\omega_i, \omega_j)$. The final alignments
 184 is then used to match the configurations. See the GitHub repository ¹ and Appendix C for alignment
 185 examples and more implementation details.

¹<https://anonymous.4open.science/r/project-82CE>

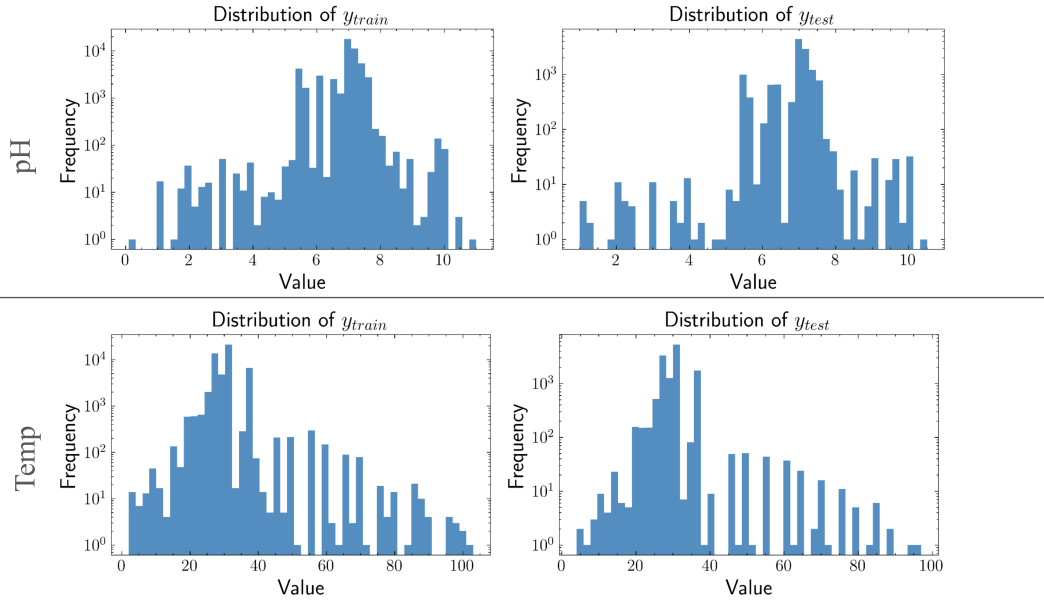


Figure 5: Illustration of target value distributions across train-test splits in DSNI dataset. The first row represents pH distributions and the second row represents temperature distributions. The first column represents the training set (y_{train}) and the second column represents the test set (y_{test}).

186 4 Experiments

187 In this section, we evaluate the proposed plug-and-play module by training baseline models with and
 188 without GraMixC (*GMC*). We also test a static variant (*GC*), which use aligned configurations as
 189 extra features, without attention mechanism. We expect the performance to follow a general trend

$$\text{baseline} < \text{baseline+GC} < \text{baseline+GMC}.$$

190 We then ablate the number of configurations used to check that they cause a performance regression.

191 4.1 Implementation details and experimental setup

192 Our module was implemented with MATLAB, Python 3.12, PyTorch 2.6. We run trainings on a
 193 GeForce RTX 3090Ti GPU. Models were trained with the Adam optimizer [34] at a fixed learning
 194 rate of 10^{-3} . Unless otherwise noted, we used a batch size of 100 and trained for up to 100 epochs.

195 Ahead of diving into the experimental details, we briefly summarize the datasets and metrics used.

196 **DSNI-pH and DSNI-Temp.** We collected the DSNI dataset from DSMZ [35] and NIH [36]. It
 197 comprises six relational tables (STRAINS, MEDIA, SOLUTIONS, INGREDIENTS, STEPS, GAS)
 198 covering taxonomic and protocol information. We use approximately 65 000 samples with 16S rRNA
 199 sequence (500–1 500 nucleotides), cultivation temperatures (2–103 °C), and pH (0.1–11). The task is
 200 to predict optimal temperature (DSNI-Temp) and pH (DSNI-pH) from the 16S rRNA sequence.

201 Following Çelikkanat, Masegosa, and Nielsen [37] and related works [38], [39], we encode each
 202 16S rRNA sequence as a 7-mer count vector in $\mathbb{N}^{16,384}$, yielding a dataset of shape $65\,023 \times 16\,384$.
 203 We perform an 80/20 split (52,018 train / 13,005 test), which preserves the skewed pH (6–8) and
 204 temperature (20–40 °C) distributions. Fig. 5 provides an illustration for target value (y_{train} and y_{test})
 205 distribution. Preprocessing—robust scaling, variance thresholding, and selection of the top 1,000
 206 features—was fitted on the training set and then applied to both splits to avoid data leakage.

207 **Additional benchmarks.** We further evaluate on QM9 [40] for molecular property regression, on
 208 Boston Housing [41], and on MNIST [42] and CIFAR10 for classification (some in Appendix D).

209 **Evaluation metrics.** For regression we use mean squared error (MSE), mean absolute error (MAE);
 210 used for QM9 for comparability with SOTA) for training, and report coefficient of determination
 211 (R^2). For classification we use cross-entropy loss (CE) for training and report top-1 accuracy (Acc).

Table 1: Regression performance on DSNI-pH, DSNI-Temp and QM9. Values are mean \pm std from runs with different random seeds; best results per baseline are bold; best results per metric are underlined.

	DSNI-pH		DSNI-Temp		QM9	
	MSE \downarrow	R ²	MSE \downarrow	R ²	MAE \downarrow	R ²
RF	0.198 \pm 0.000	0.601 \pm 0.001	17.759 \pm 0.276	0.393 \pm 0.009	0.015 \pm 0.000	0.979 \pm 0.000
XGBoost	0.196 \pm 0.001	0.604 \pm 0.003	18.212 \pm 0.543	0.377 \pm 0.018	0.014 \pm 0.001	0.978 \pm 0.001
CatBoost	0.193 \pm 0.001	0.610 \pm 0.002	17.375 \pm 0.398	0.406 \pm 0.013	0.014 \pm 0.000	0.978 \pm 0.002
3LP	0.201 \pm 0.002	0.595 \pm 0.006	18.484 \pm 0.183	0.368 \pm 0.006	0.018 \pm 0.001	0.958 \pm 0.001
3LP+GC	0.097 \pm 0.004	0.804 \pm 0.008	6.520 \pm 0.360	0.777 \pm 0.012	0.016 \pm 0.003	0.974 \pm 0.000
3LP+GMC	0.023 \pm 0.002	0.953 \pm 0.004	2.277 \pm 0.061	0.922 \pm 0.002	0.010 \pm 0.003	0.990 \pm 0.002
TabN	0.184 \pm 0.004	0.629 \pm 0.007	13.290 \pm 0.244	0.545 \pm 0.008	0.015 \pm 0.001	0.962 \pm 0.002
TabN+GC	0.086 \pm 0.003	0.825 \pm 0.007	7.997 \pm 0.210	0.726 \pm 0.007	0.012 \pm 0.002	0.983 \pm 0.001
TabN+GMC	0.020 \pm 0.001	0.959 \pm 0.002	0.989 \pm 0.361	0.966 \pm 0.012	0.008 \pm 0.000	0.995 \pm 0.002
TabT	0.256 \pm 0.007	0.483 \pm 0.014	18.910 \pm 0.247	0.353 \pm 0.008	0.434 \pm 0.008	0.921 \pm 0.008
TabT+GC	0.106 \pm 0.002	0.786 \pm 0.005	8.280 \pm 0.303	0.717 \pm 0.010	0.212 \pm 0.004	0.961 \pm 0.008
TabT+GMC	0.017 \pm 0.002	0.964 \pm 0.005	2.785 \pm 0.540	0.904 \pm 0.018	0.009 \pm 0.000	0.998 \pm 0.001
FTT	0.218 \pm 0.003	0.561 \pm 0.006	13.571 \pm 0.069	0.536 \pm 0.002	0.085 \pm 0.005	0.984 \pm 0.006
FTT+GC	0.070 \pm 0.003	0.858 \pm 0.007	5.915 \pm 0.277	0.797 \pm 0.009	0.034 \pm 0.002	0.993 \pm 0.003
FTT+GMC	0.007 \pm 0.005	0.984 \pm 0.009	1.480 \pm 0.120	0.949 \pm 0.004	0.026 \pm 0.001	0.995 \pm 0.003

212 For each benchmark, we include three classical decision tree models for reference: Random Forest
213 (RF) [43], XGBoost [44], CatBoost [45]. As both GMC and GC are plug-and-play modules, they can
214 be easily applied to various downstream predictors. We first evaluate a 3-layer perceptron (3LP) with
215 hidden dims [256,128,64]. Because our inputs combine numerical features with categorical config-
216urations, we naturally consider tabular models: TabNet (TabN) [46], TabTransformer (TabT) [47],
217 FT-Transformer (FTT) [48] were all run with their default settings from the official implementations.

218 4.2 Evaluation of the proposed module

219 As shown in Fig. 2 and Fig. 3, we demonstrate, with attention maps, the learned mixing of config-
220urations by training models with self-attention head on aligned configurations. In order to quantify
221 the quality of such mixing, for each baseline, we set up the evaluation in three modes: standalone
222 (baseline), with static configuration concatenation (baseline+GC), and with attention-based fusion via
223 GraMixC (baseline+GMC). Table 1 reports regression results on our main benchmarks; Appendix D
224 (Table 2) shows the rest results. Across all models and tasks, adding GC yields consistent gains, and
225 incorporating GMC provides further significant improvements, confirming our initial hypothesis.

226 **Performance improvement.** Table 1 shows that adding GC and GMC yields consistent gains across
227 all baselines. Among these observed improvements, the scores increasing on DSNI is quite satisfying.
228 Prior specialized growth-media regression methods are not convincing with $R^2 \leq 0.8$ (e.g., 0.75 [49]).
229 We confirm this with our base models score R^2 between 0.3 and 0.6 on DSNI-pH and DSNI-Temp.
230 However, even without tailoring the baseline model design, we bring the score to a new high by
231 simply adding GC or GMC. Fig. 6 illustrates some examples of such improvement. We see the
232 model’s predictions align more closely with the ideal regression line and better handle rare cases,
233 by incorporating configurations and probably capturing the latent manifold structure. Incorporating
234 GC and further GMC raises R^2 to 0.98 (pH) and 0.97 (Temp). Which not only is considered very
235 satisfying in application of bacterial cultivation but also set the new state-of-the-art (SOTA) for
236 growth-media prediction. On QM9, GraMixC achieves an MAE of 0.008, nearly matching the SOTA
237 (w/o extra training data) of 0.007 [50], and represents the best result among non-GNN models.

238 **Number of configurations used.** We ablate the number of configuration levels in GMC. Fig. 7 shows
239 that more configurations generally decreases MSE and increases R^2 , confirming the value of multi-
240 resolution information. Importantly, GMC often needs more than half as many total configurations to
241 outperform GC, and performance plateaus—or even slightly declines—when including the last few

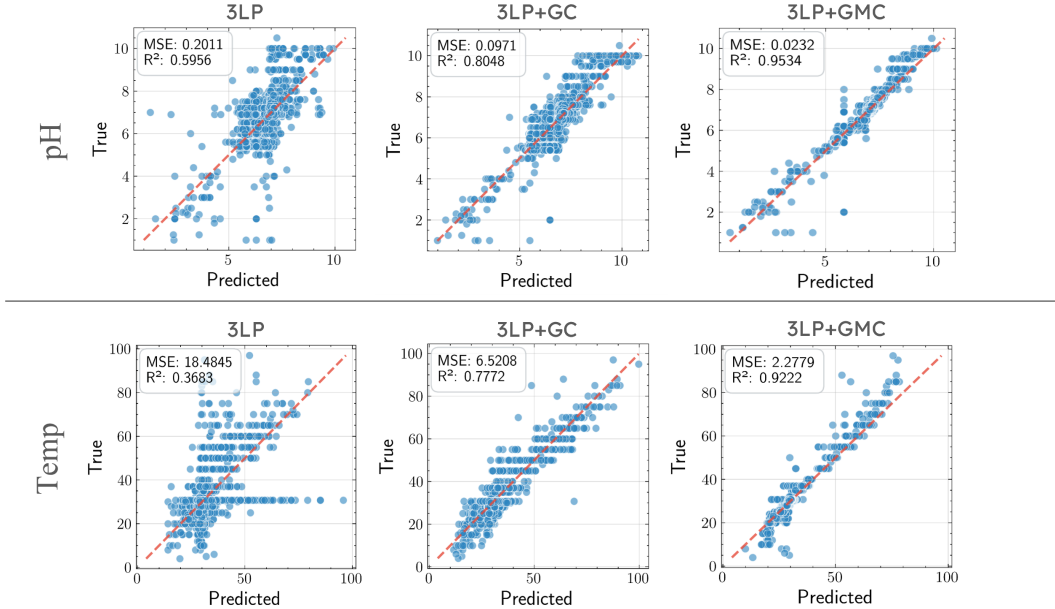


Figure 6: Illustration of the regression performance improvement example in 3LP by adding GC or GMC. Each column plots predicted vs. actual pH (top) or temperature (bottom). 3LP+GC (middle) outperforms the 3LP baseline (left), while 3LP+GMC (right) further boosts R^2 up to > 0.9 .

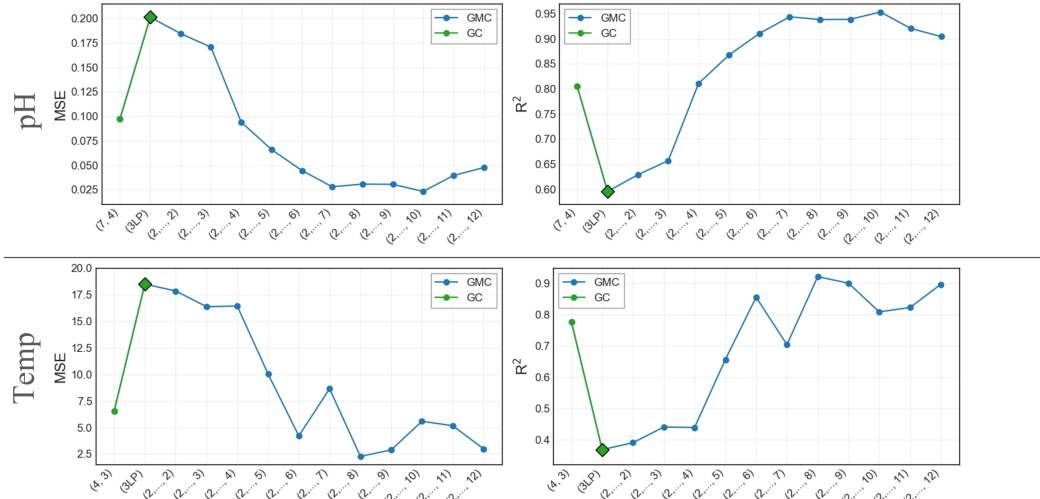
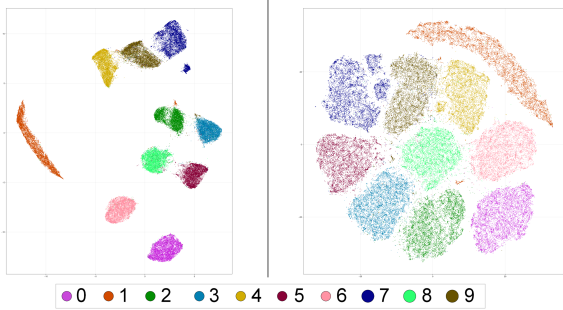


Figure 7: Ablation study on the number of configurations used on DSNI. On the blue curves (GMC), $[2, \dots, i]$ denote fusing configurations from 2 through i via GraMixC. On the green curves (GC), (i, j) denote the best train/test configuration pair used in static concatenation. Incrementally mixing configurations improves performance and outperforms static concatenation.

242 configurations. These aligns with Pitsianis et al. [8], who report a finite set of optimal configurations
243 rather than continuous gains at infinite resolutions. Using all configurations available is still preferred.

244 4.3 Qualitative evaluation of configurations.

245 Our final experiment compares configurations against standard representation-extraction methods. As
246 discussed in Section 1, configurations can be viewed as special unsupervised representation learning.
247 Fig. 3 already shows their advantage over self-supervised register tokens. Here, we replace GC/GMC
248 with PCA [51], UMAP [52], and a vanilla autoencoder (AE), each embed into dimensions the same



(a) 2D visualization of embeddings learned.

	CE ↓	Acc
3LP+PCA	0.157	0.971
3LP+UMAP	0.181	0.975
3LP+AE	0.158	0.969
3LP+GC	0.046	0.992
3LP+GMC	0.028	0.993

(b) Classification performance.

Figure 8: (a): Illustration of 2D embeddings of MNIST using UMAP (left) and SG-t-SNE (right). (b): Classification performance on MNIST using features from PCA, UMAP, autoencoder (AE), static configurations (GC), and GraMixC (GMC) at equal embedding dimensions. SG-t-SNE embeddings integrated via GC or GMC exploit multi-resolution structure to notably outperform other methods.

249 number of as our configurations. We visualize these embeddings on MNIST (Fig. 8a; additional
 250 views in Appendix D.2). Qualitatively, SG-t-SNE (the reduction step in GraMixC) yields more
 251 uniform, well-separated clusters that respect global kNN connectivity rather than forming hubs.
 252 Fig. 8b quantifies downstream classification accuracy, where GC and GMC strongly outperform PCA,
 253 UMAP, and AE given the same embedding budget. These results confirm that mixed configurations
 254 provide a more expressive yet compact representation for downstream tasks.

255 5 Conclusion

256 In this study, we investigate the functional mechanisms of configurations in downstream prediction
 257 tasks and identify three key properties. Based on this, we propose GraMixC, which dynamically
 258 mixes configurations through attention head. We apply it to the challenging task of 16S rRNA
 259 cultivation-media prediction task, and set a new state-of-the-art. Further validation across multiple
 260 standard tabular data benchmarks consistently reveals that GC (a static version of GraMixC) enhances
 261 baseline performance, while GraMixC demonstrates even more substantial improvements. Our results
 262 suggest that harnessing rich manifold priors via attention-driven fusion opens promising avenues for
 263 interpretable and robust learning in both scientific and conventional domains.

264 In future work, we plan to extend mixed configurations to more expressive networks and dynamically
 265 learn configuration alignment through end-to-end differentiable modules. Additionally, we will focus
 266 on exploring adaptive clustering for evolving data streams where train and test distributions may shift,
 267 which could further enhance the resilience of multi-resolution approaches.

268 References

- 269 [1] J. MacQueen. “Some Methods for Classification and Analysis of Multivariate Observations”.
 270 In: *Proceedings of the Fifth Berkeley Symposium on Mathematical Statistics and Probability, Volume 1: Statistics*. Vol. 5.1. University of California Press, Jan. 1, 1967, pp. 281–298.
- 272 [2] Jianbo Shi and J. Malik. “Normalized Cuts and Image Segmentation”. In: *IEEE Trans. Pattern Anal. Machine Intell.* 22.8 (Aug. 2000), pp. 888–905.
- 274 [3] A. Ng, M. Jordan, and Y. Weiss. “On Spectral Clustering: Analysis and an Algorithm”. In:
 275 *Advances in Neural Information Processing Systems*. Vol. 14. MIT Press, 2001.
- 276 [4] P. C. Quinn and P. D. Eimas. “Perceptual Cues That Permit Categorical Differentiation of
 277 Animal Species by Infants”. In: *J Exp Child Psychol* 63.1 (Oct. 1996), pp. 189–211. PMID:
 278 8812045.
- 279 [5] M. H. Bornstein, M. E. Arterberry, and C. Mash. “Infant Object Categorization Transcends
 280 Diverse Object-Context Relations”. In: *Infant Behav Dev* 33.1 (Feb. 2010), pp. 7–15. PMID:
 281 20031232.

- 282 [6] L. Zaadnoordijk, T. R. Besold, and R. Cusack. “Lessons from Infant Learning for Unsupervised
283 Machine Learning”. In: *Nat Mach Intell* 4.6 (June 2022), pp. 510–520.
- 284 [7] L. Muttenthaler, K. Greff, F. Born, B. Spitzer, S. Kornblith, M. C. Mozer, K.-R. Müller, T.
285 Unterthiner, and A. K. Lampinen. *Aligning Machine and Human Visual Representations across*
286 *Abstraction Levels*. Oct. 29, 2024. arXiv: 2409 . 06509 [cs]. URL: <http://arxiv.org/abs/2409.06509> (visited on 05/11/2025). Pre-published.
- 288 [8] N. Pitsianis, D. Floros, T. Liu, and X. Sun. “Parallel Clustering with Resolution Variation”.
289 In: *2023 IEEE High Performance Extreme Computing Conference (HPEC)*. 2023 IEEE High
290 Performance Extreme Computing Conference (HPEC). Boston, MA, USA: IEEE, Sept. 25,
291 2023, pp. 1–8.
- 292 [9] A. Krizhevsky. *Learning Multiple Layers of Features from Tiny Images*. Toronto, ON, Canada,
293 2009, pp. 32–33.
- 294 [10] J. M. Janda and S. L. Abbott. “16S rRNA Gene Sequencing for Bacterial Identification in the
295 Diagnostic Laboratory: Pluses, Perils, and Pitfalls”. In: *J Clin Microbiol* 45.9 (Sept. 2007),
296 pp. 2761–2764. PMID: 17626177.
- 297 [11] Q. Wang, G. M. Garrity, J. M. Tiedje, and J. R. Cole. “Naive Bayesian Classifier for Rapid
298 Assignment of rRNA Sequences into the New Bacterial Taxonomy”. In: *Appl Environ Microbiol*
299 73.16 (Aug. 2007), pp. 5261–5267. PMID: 17586664.
- 300 [12] J. De Vrieze, A. J. Pinto, W. T. Sloan, and U. Z. Ijaz. “The Active Microbial Community
301 More Accurately Reflects the Anaerobic Digestion Process: 16S rRNA (Gene) Sequencing as
302 a Predictive Tool”. In: *Microbiome* 6.1 (Apr. 2, 2018), p. 63.
- 303 [13] J. S. Johnson, D. J. Spakowicz, B.-Y. Hong, L. M. Petersen, P. Demkowicz, L. Chen, S. R.
304 Leopold, B. M. Hanson, H. O. Agresta, M. Gerstein, E. Sodergren, and G. M. Weinstock.
305 “Evaluation of 16S rRNA Gene Sequencing for Species and Strain-Level Microbiome Analysis”.
306 In: *Nat Commun* 10.1 (Nov. 6, 2019), p. 5029.
- 307 [14] M. Caron, P. Bojanowski, A. Joulin, and M. Douze. *Deep Clustering for Unsupervised Learning*
308 *of Visual Features*. Version 2. Mar. 18, 2019. arXiv: 1807 . 05520 [cs]. URL: <http://arxiv.org/abs/1807.05520> (visited on 05/13/2025). Pre-published.
- 310 [15] Y. Yang, Z. Guan, Z. Wang, W. Zhao, C. Xu, W. Lu, and J. Huang. *Self-Supervised Heteroge-*
311 *neous Graph Pre-training Based on Structural Clustering*. Apr. 12, 2023. arXiv: 2210 . 10462
312 [cs]. URL: <http://arxiv.org/abs/2210.10462> (visited on 05/13/2025). Pre-published.
- 313 [16] T. Dariset, M. Oquab, J. Mairal, and P. Bojanowski. *Vision Transformers Need Registers*.
314 Apr. 12, 2024. arXiv: 2309 . 16588 [cs]. URL: <http://arxiv.org/abs/2309.16588>
315 (visited on 03/25/2025). Pre-published.
- 316 [17] F. Locatello, D. Weissenborn, T. Unterthiner, A. Mahendran, G. Heigold, J. Uszkoreit, A.
317 Dosovitskiy, and T. Kipf. *Object-Centric Learning with Slot Attention*. Oct. 14, 2020. arXiv:
318 2006 . 15055 [cs]. URL: <http://arxiv.org/abs/2006.15055> (visited on 05/11/2025).
319 Pre-published.
- 320 [18] M. Caron, H. Touvron, I. Misra, H. Jégou, J. Mairal, P. Bojanowski, and A. Joulin. *Emerging*
321 *Properties in Self-Supervised Vision Transformers*. May 24, 2021. arXiv: 2104 . 14294 [cs].
322 URL: <http://arxiv.org/abs/2104.14294> (visited on 03/25/2025). Pre-published.
- 323 [19] M. Oquab, T. Dariset, T. Moutakanni, H. Vo, M. Szafraniec, V. Khalidov, P. Fernandez, D.
324 Haziza, F. Massa, A. El-Nouby, M. Assran, N. Ballas, W. Galuba, R. Howes, P.-Y. Huang,
325 S.-W. Li, I. Misra, M. Rabbat, V. Sharma, G. Synnaeve, H. Xu, H. Jegou, J. Mairal, P. Labatut,
326 A. Joulin, and P. Bojanowski. *DINOv2: Learning Robust Visual Features without Supervision*.
327 Feb. 2, 2024. arXiv: 2304 . 07193 [cs]. URL: <http://arxiv.org/abs/2304.07193>
328 (visited on 03/25/2025). Pre-published.
- 329 [20] O. Siméoni, G. Puy, H. V. Vo, S. Roburin, S. Gidaris, A. Bursuc, P. Pérez, R. Marlet, and
330 J. Ponce. *Localizing Objects with Self-Supervised Transformers and No Labels*. Sept. 29,
331 2021. arXiv: 2109 . 14279 [cs]. URL: <http://arxiv.org/abs/2109.14279> (visited on
332 03/25/2025). Pre-published.
- 333 [21] H. Zhang, F. Li, S. Liu, L. Zhang, H. Su, J. Zhu, L. M. Ni, and H.-Y. Shum. *DINO: DETR with*
334 *Improved DeNoising Anchor Boxes for End-to-End Object Detection*. July 11, 2022. arXiv:
335 2203 . 03605 [cs]. URL: <http://arxiv.org/abs/2203.03605> (visited on 03/25/2025).
336 Pre-published.

- 337 [22] A. Vaswani, N. Shazeer, N. Parmar, J. Uszkoreit, L. Jones, A. N. Gomez, Łukasz Kaiser, and
 338 I. Polosukhin. “Attention Is All You Need”. In: *Advances in Neural Information Processing*
 339 *Systems*. Vol. 30. Curran Associates, Inc., 2017.
- 340 [23] T. Liu, D. Floros, N. Pitsianis, and X. Sun. “Digraph Clustering by the BlueRed Method”.
 341 In: *2021 IEEE High Performance Extreme Computing Conference (HPEC)*. 2021 IEEE High
 342 Performance Extreme Computing Conference (HPEC). Sept. 2021, pp. 1–7.
- 343 [24] J. B. Tenenbaum, V. de Silva, and J. C. Langford. “A Global Geometric Framework for
 344 Nonlinear Dimensionality Reduction”. In: *Science* 290.5500 (Dec. 22, 2000), pp. 2319–2323.
- 345 [25] N. Pitsianis, A.-S. Iliopoulos, D. Floros, and X. Sun. “Spaceland Embedding of Sparse
 346 Stochastic Graphs”. In: *2019 IEEE High Performance Extreme Computing Conference (HPEC)*.
 347 2019 IEEE High Performance Extreme Computing Conference (HPEC). Sept. 2019, pp. 1–8.
- 348 [26] L. Van der Maaten and G. Hinton. “Visualizing Data Using T-SNE.” In: *Journal of machine*
 349 *learning research* 9.11 (2008), pp. 2579–2605.
- 350 [27] V. A. Traag, L. Waltman, and N. J. Van Eck. “From Louvain to Leiden: Guaranteeing Well-
 351 Connected Communities”. In: *Sci. Rep.* 9.1 (Mar. 26, 2019), p. 5233.
- 352 [28] L. J. Hubert and P. Arabie. “Comparing Partitions”. In: *Journal of Classification* 2.2–3 (1985),
 353 pp. 193–218.
- 354 [29] H. W. Kuhn. “The Hungarian Method for the Assignment Problem”. In: *Nav. Res. Logist. Q.*
 355 2.1–2 (Mar. 1955), pp. 83–97.
- 356 [30] R. Jonker and A. Volgenant. “A Shortest Augmenting Path Algorithm for Dense and Sparse
 357 Linear Assignment Problems”. In: *Computing* 38.4 (Dec. 1, 1987), pp. 325–340.
- 358 [31] D. P. Bertsekas. “Auction Algorithms for Network Flow Problems: A Tutorial Introduction”.
 359 In: *Comput Optim Applic* 1.1 (Oct. 1992), pp. 7–66.
- 360 [32] M. Fiedler. “Algebraic Connectivity of Graphs”. In: *Czech. Math. J.* 23.2 (1973), pp. 298–305.
- 361 [33] D. Floros, N. Pitsianis, and X. Sun. “Algebraic Vertex Ordering of a Sparse Graph for Adjacency
 362 Access Locality and Graph Compression”. In: *2024 IEEE High Performance Extreme*
 363 *Computing Conference (HPEC)*. 2024 IEEE High Performance Extreme Computing Conference
 364 (HPEC). Sept. 2024, pp. 1–7.
- 365 [34] D. P. Kingma and J. Ba. “Adam: A Method for Stochastic Optimization”. In: *arXiv:1412.6980*
 366 [*cs.LG*] (Jan. 30, 2017). arXiv: 1412.6980 [*cs.LG*].
- 367 [35] German Collection of Microorganisms and Cell Cultures GmbH. *DSMZ – German Collection*
 368 *of Microorganisms and Cell Cultures*. 2025.
- 369 [36] National Institutes of Health (NIH). National Institutes of Health (NIH). URL: <https://www.nih.gov/> (visited on 02/04/2025).
- 370 [37] A. Çelikkınat, A. R. Masegosa, and T. D. Nielsen. “Revisiting K-mer Profile for Effective and
 371 Scalable Genome Representation Learning”. In: () .
- 372 [38] *Kraken: Ultrafast Metagenomic Sequence Classification Using Exact Alignments* | *Genome*
 373 *Biology* | *Full Text*. URL: <https://genomebiology.biomedcentral.com/articles/10.1186/gb-2014-15-3-r46> (visited on 02/04/2025).
- 374 [39] *How to Apply de Bruijn Graphs to Genome Assembly* | *Nature Biotechnology*. URL: <https://www.nature.com/articles/nbt.2023> (visited on 02/04/2025).
- 375 [40] R. Ramakrishnan, P. O. Dral, M. Rupp, and O. A. von Lilienfeld. “Quantum Chemistry
 376 Structures and Properties of 134 Kilo Molecules”. In: *Sci Data* 1.1 (Aug. 5, 2014), p. 140022.
- 377 [41] D. Harrison and D. L. Rubinfeld. “Hedonic Housing Prices and the Demand for Clean Air”.
 378 In: *Journal of Environmental Economics and Management* 5.1 (Mar. 1, 1978), pp. 81–102.
- 379 [42] Y. Lecun, L. Bottou, Y. Bengio, and P. Haffner. “Gradient-Based Learning Applied to Docu-
 380 ment Recognition”. In: *Proceedings of the IEEE* 86.11 (Nov. 1998), pp. 2278–2324.
- 381 [43] L. Breiman. “Random Forests”. In: *Machine Learning* 45.1 (2001), pp. 5–32.
- 382 [44] T. Chen and C. Guestrin. “XGBoost: A Scalable Tree Boosting System”. In: *Proceedings of*
 383 *the 22nd ACM SIGKDD International Conference on Knowledge Discovery and Data Mining*.
 384 Aug. 13, 2016, pp. 785–794. arXiv: 1603.02754 [*cs.LG*].
- 385 [45] L. Prokhorenkova, G. Gusev, A. Vorobev, A. V. Dorogush, and A. Gulin. “CatBoost: Unbiased
 386 Boosting with Categorical Features”. In: *Advances in Neural Information Processing Systems*.
 387 Vol. 31. Curran Associates, Inc., 2018.

- 391 [46] S. O. Arik and T. Pfister. *TabNet: Attentive Interpretable Tabular Learning*. Dec. 9, 2020. arXiv:
 392 1908.07442 [cs]. URL: <http://arxiv.org/abs/1908.07442> (visited on 05/14/2025).
 393 Pre-published.
- 394 [47] X. Huang, A. Khetan, M. Cvitkovic, and Z. Karnin. *TabTransformer: Tabular Data Modeling
 395 Using Contextual Embeddings*. Dec. 11, 2020. arXiv: 2012.06678 [cs]. URL: <http://arxiv.org/abs/2012.06678> (visited on 05/05/2025). Pre-published.
- 396 [48] Y. Gorishniy, I. Rubachev, V. Khrulkov, and A. Babenko. *Revisiting Deep Learning Models
 397 for Tabular Data*. Oct. 26, 2023. arXiv: 2106.11959 [cs]. URL: <http://arxiv.org/abs/2106.11959> (visited on 05/14/2025). Pre-published.
- 398 [49] D. B. Sauer and D.-N. Wang. “Predicting the Optimal Growth Temperatures of Prokaryotes
 399 Using Only Genome Derived Features”. In: *Bioinformatics* 35.18 (Sept. 15, 2019), pp. 3224–
 400 3231.
- 401 [50] X. Fang, L. Liu, J. Lei, D. He, S. Zhang, J. Zhou, F. Wang, H. Wu, and H. Wang. “Geometry-
 402 Enhanced Molecular Representation Learning for Property Prediction”. In: *Nat Mach Intell*
 403 4.2 (Feb. 2022), pp. 127–134.
- 404 [51] *Principal Component Analysis*. Springer Series in Statistics. New York: Springer-Verlag, 2002.
- 405 [52] L. McInnes, J. Healy, and J. Melville. “UMAP: Uniform Manifold Approximation and Pro-
 406 jection for Dimension Reduction”. In: *arXiv:1802.03426 [stat.ML]* (Sept. 18, 2020). arXiv:
 407 1802.03426 [stat.ML].
- 408
- 409

410 A An Intuitive Example of Configuration Mixing

411 To illustrate the necessity of fusing valid clusterings across resolution scales, we use two synthetic
 412 point-cloud datasets from scikit-learn: “Moons” and “Blobs.” The Blobs dataset is tuned so that no
 413 single clustering resolution recovers all three clusters. Fig. 9 visualizes each dataset in 3D, using the
 414 third axis to encode cluster assignments for corresponding configuration: coarser configuration (1)
 415 and finer configuration (2). Configuration (1), by lifting some dots above the plane, cleanly separates
 416 the two Moon arcs but merges two (purple and green) of the Blobs clusters. Configuration (2), by
 417 itself, fails the Blobs with a different merge (blue and green). Only by fusing both configurations
 418 can all clusters be disentangled—the purple dots in (1) that falls down in (2), emerges correct as the
 419 green cluster. This toy example shows that multi-resolution clusterings alone are insufficient without
 420 a fusion mechanism. Our GraMixC use attention-based fusion to integrate these scales. While just
 421 one demonstration, it highlights the broader advantage of mixing configurations in complex settings.

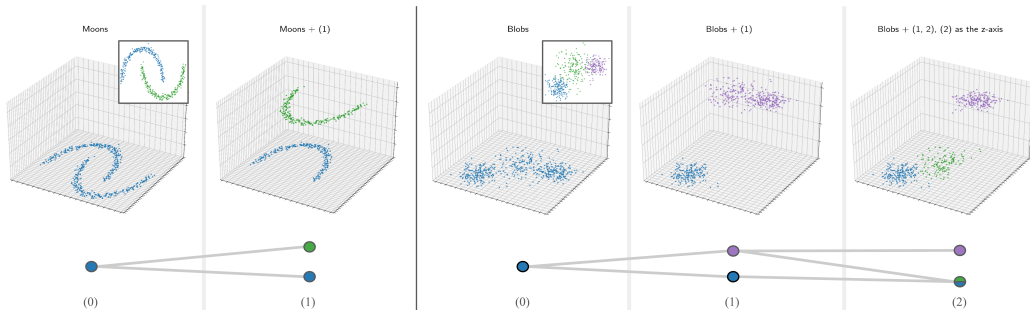


Figure 9: Illustration of multi-resolution clustering on synthetic datasets. GT is shown in the framed box in (0). Upper is the embedding of Moons (left) and Blobs (right) with corresponding configuration (i) as third dimension; lower is lineage diagram of the configurations.

422 B Synthetic Clustering Benchmarks

423 In this section, we further discuss the limitations of conventional clustering methods raised in
 424 Section 3.1. We compare our modularity-based clustering strategy, which is used as the unsupervised
 425 layer in GraMixC, against widely-used clustering algorithms on synthetic 2D datasets.

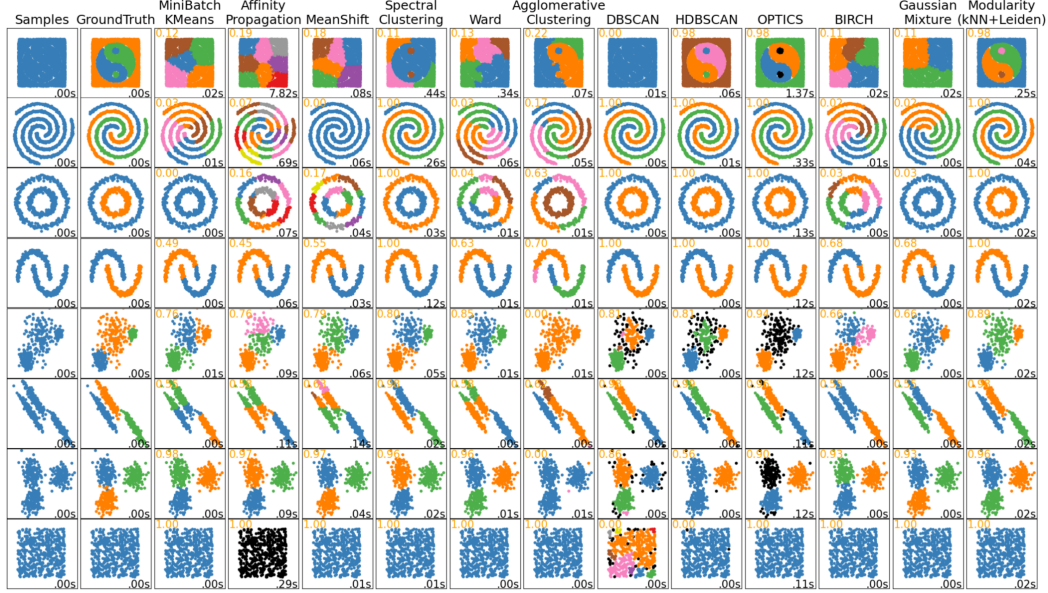


Figure 10: Illustration of clustering methods comparisons across multiple synthetic datasets. Rows correspond to different 2D point clouds—first row is custom, others from scikit-learn. Each method’s result is labeled with ARI (top-left in yellow) and execution time (bottom-right in black). *Modularity: kNN+Leiden* (far right) accurately recovers ground-truth structures across different shapes and densities, with robustness to noise, anisotropy, and distribution variation.

- 426 Each row in Fig. 10 presents a distinct synthetic dataset distribution, ranging from custom-designed
 427 to standard scikit-learn datasets, including *Taiji*, spirals, circles, moons, varied blobs, anisotropy,
 428 blobs, and isotropic noise. Each column represents the result of one clustering method, annotated
 429 with Adjusted Rand Index (ARI) and execution time.
 430 Unlike traditional clustering methods, the approach we adopted (last column: Modularity, im-
 431 plemented via kNN graph + Leiden community detection) consistently uncovers the underlying
 432 structure—even in challenging cases involving non-convex geometries, anisotropic spreads, or un-
 433 even density distributions. This comparison underscores the reliability and manifold sensitivity of our
 434 unsupervised segmentation approach, even before introducing multi-resolution fusion or downstream
 435 learning tasks.

436 C RMS Alignment Details

437 In Section 3.2 we introduced the Reverse Merge & Split (RMS) procedure for aligning multi-
 438 resolution configurations between train and test sets. Below we provide the full pseudo-code in
 439 Algorithm 1, using the same notation as the main text.

440 Implementation notes.

- 441 • We set $\theta = 0.1$ and compute ARI as in Hubert and Arabie [28].
 442 • We use 0.1 % of the train samples as anchors to form \mathcal{A} .
 443 • The greedy matching loops over each train configuration ω_i to find its best-scoring test
 444 partner ω_j , applies the label mapping, and removes both from further consideration to ensure
 445 one-to-one alignment.

446 The details for SCORE and L_{tw} are covered in Algorithm 1 so we skip them here.

Algorithm 1 Reverse Merge & Split (RMS) Alignment

Require: $\Omega_{\text{train}} \in \mathbb{N}^{N \times m_t}$, $\Omega_{\text{test}} \in \mathbb{N}^{N \times m_s}$, anchor indices $\mathcal{A} \subset \{1, \dots, N\}$, θ

Ensure: Aligned Ω_{test}

```
1:  $\mathbb{U} \leftarrow \{1, \dots, m_t\}$ ,  $\mathbb{V} \leftarrow \{1, \dots, m_s\}$ 
2: for  $i$  in  $\mathbb{U}$  do ▷ for each train configuration  $\omega_i$ 
3:   best_score  $\leftarrow -\infty$ , best_j  $\leftarrow \text{null}$ 
4:    $\omega_i \leftarrow \Omega_{\text{train}}[\mathcal{A}, i]$ 
5:   for  $j$  in  $\mathbb{V}$  do ▷ find best test configuration  $\omega_j$ 
6:      $\omega_j \leftarrow \Omega_{\text{test}}[\mathcal{A}, j]$ 
7:      $s \leftarrow \text{SCORE}(\omega_i, \omega_j, \theta)$ 
8:     if  $s > \text{best\_score}$  then
9:       best_score  $\leftarrow s$ , best_j  $\leftarrow j$ 
10:    end if
11:   end for
12:    $M \leftarrow \text{PAIR\_MAPPING}(\Omega_{\text{train}}[:, i], \Omega_{\text{test}}[:, \text{best\_j}])$ 
13:   for  $p = 1$  to  $N$  do
14:      $\Omega_{\text{test}}[p, \text{best\_j}] \leftarrow M(\Omega_{\text{test}}[p, \text{best\_j}])$ 
15:   end for
16:   Remove  $i$  from  $\mathbb{U}$ , remove best_j from  $\mathbb{V}$ 
17: end for
18: return  $\Omega_{\text{test}}$ 

19: function PAIR_MAPPING( $\omega_i, \omega_j$ )
20:    $n_i \leftarrow \|\omega_i\|_\infty$ ,  $n_j \leftarrow \|\omega_j\|_\infty$ 
21:   for  $p = 1$  to  $N$  do ▷ build confusion matrix  $C \in \mathbb{N}^{n_i \times n_j}$ 
22:      $C[\omega_i[p], \omega_j[p]] += 1$ 
23:   end for
24:   Construct two-walk Laplacian  $L_{\text{tw}}$ 
25:    $\mathcal{F} \leftarrow \text{Fiedler vector of } L_{\text{tw}}$ 
26:   Split  $\mathcal{F} \rightarrow (\mathcal{F}_i \in \mathbb{R}^{n_i}, \mathcal{F}_j \in \mathbb{R}^{n_j})$ 
27:    $\pi_i \leftarrow \text{argsort}(\mathcal{F}_i)$ ,  $\pi_j \leftarrow \text{argsort}(\mathcal{F}_j)$ 
28:   return mapping  $k \mapsto \pi_i[\pi_j^{-1}(k)]$  for  $k = 1, \dots, \min(n_i, n_j)$ 
29: end function
```

447 **D Additional Experimental Results**448 In Section 4 we introduced our experimental setup and high-level results. Here, we provide the full
449 details and qualitative analyses that couldn't fit into the main body, including:

- 450 • Downstream task performance on three other benchmarks.
-
- 451 • Qualitative illustration of prediction versus true value on the three tabular baseline models.
-
- 452 • Embeddings from PCA and AE.

453 **D.1 Additional evaluation of proposed module**454 Table 2 extends our evaluation to three additional benchmarks: Boston Housing (regression), MNIST
455 and CIFAR-10 (classification). We compare classical ensembles (RF, XGBoost, CatBoost), a 3-layer
456 MLP (3LP), and three neural tabular architectures (TabNet, TabTransformer, FT-Transformer) in
457 three modes: baseline, static configuration concatenation (GC), and attention-based fusion (GMC).458 Across almost all models and datasets, GC consistently improves performance over the raw baselines,
459 and GMC provides further gains.460 The sole exception is TabTransformer on Boston Housing, where GC yields only a marginal R^2
461 increase ($0.811 \rightarrow 0.813$), but GMC degrades it (to 0.671), suggesting that attention-based fusion may
462 disrupt already well-structured features in this case.463 On MNIST, GC lifts accuracy above 99%, and GMC pushes it to 99.3–99.5%. On CIFAR-10, GC
464 delivers dramatic gains (e.g. TabTransformer from 46.3% to 87.6%), and GMC further improves

Table 2: Regression/classification performance on Boston Housing (BHouse), MNIST, and CIFAR10.

Dataset	BHouse		MNIST		CIFAR10	
	Metric	MSE ↓	R ²	CE ↓	Acc	CE ↓
RF	0.022	0.884	0.247	0.969	1.681	0.463
XGBoost	0.022	0.881	0.066	0.980	1.296	0.539
CatBoost	0.016	0.913	0.096	0.975	1.230	0.567
3LP	0.023	0.879	0.141	0.970	1.428	0.524
3LP+GC	0.022	0.882	0.046	0.992	0.480	0.844
3LP+GMC	0.017	0.909	0.028	0.993	0.220	0.949
TabN	0.033	0.822	0.130	0.964	1.499	0.463
TabN+GC	0.021	0.888	0.225	0.941	0.377	0.876
TabN+GMC	0.012	0.936	0.017	0.995	0.077	0.978
TabT	0.035	0.811	0.192	0.980	1.028	0.706
TabT+GC	0.035	0.813	0.040	0.993	1.049	0.704
TabT+GMC	0.061	0.671	0.018	0.994	0.458	0.911
FTT	0.032	0.826	0.098	0.980	0.415	0.874
FTT+GC	0.030	0.838	0.029	0.993	0.437	0.870
FTT+GMC	0.026	0.860	0.018	0.995	0.157	0.955

465 all models, with FT-Transformer+GMC reaching 95.5% accuracy. These results underscore that
466 configuration integration via GraMixC is broadly effective, with only one minor counterexample.

467 D.2 Additional qualitative evaluation of configurations

468 In Section 4.3 we provided the embedding of MNIST digits using UMAP and SG-t-SNE (Fig. 8a).
469 Here we provides the missing illustration of embedding with PCA and autoencoder (AE) in Fig. 11.
470 As expected, they do not provide representation with clusters as separated as the former two methods.
471 With the final figure (Fig. 12) we visualize predicted vs. actual values from the tabular baselines on
472 DSNI, filling in what is missing from Fig. 6.

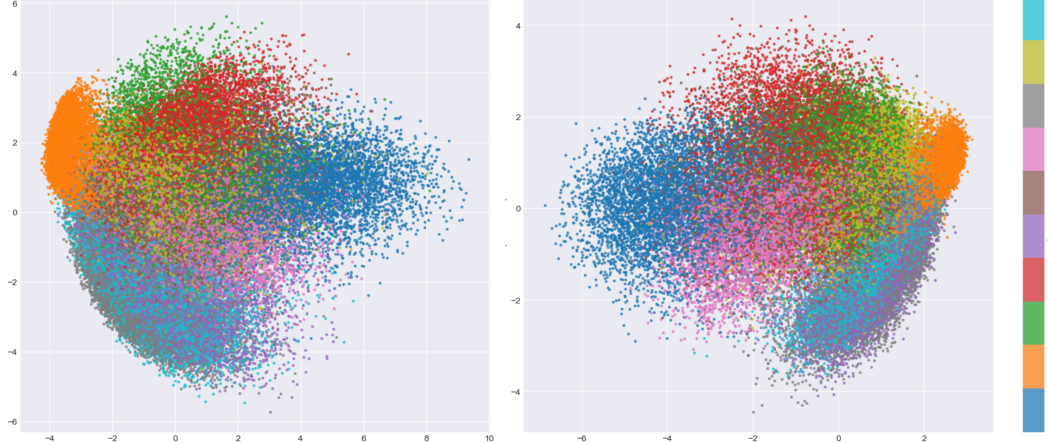


Figure 11: Illustration of 2D embeddings learned by PCA (left) and AE (right) on MNIST.

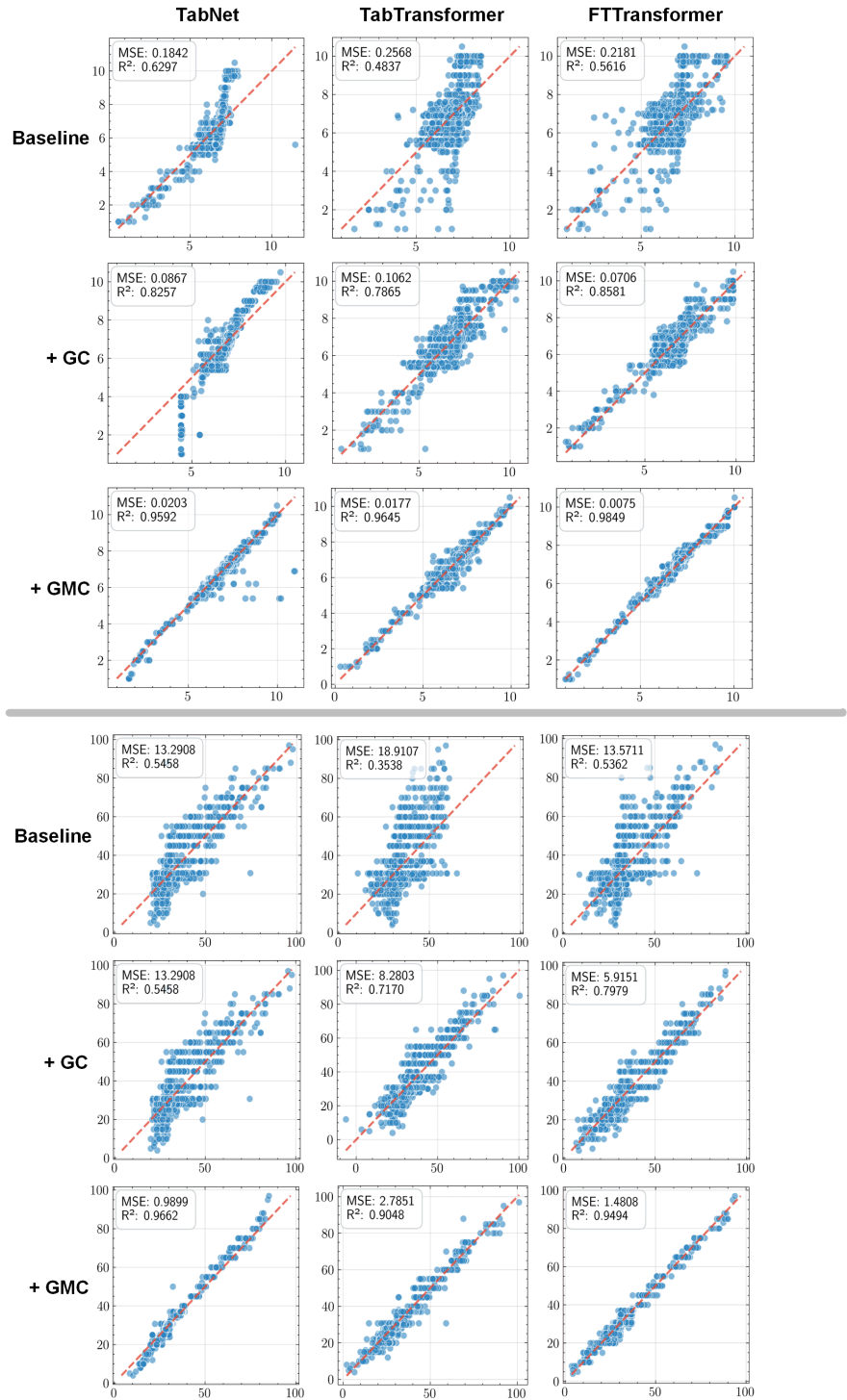


Figure 12: Illustration of the regression performance improvement example in TabNet, TabTransformer and FT-Transformer by adding GC or GMC. Each plots predicted vs. actual value.

473 **NeurIPS Paper Checklist**

474 **1. Claims**

475 Question: Do the main claims made in the abstract and introduction accurately reflect the
476 paper's contributions and scope?

477 Answer: [Yes]

478 Justification: In the abstract and introduction, we outline configuration characteristics and
479 propose GraMixC. We detail our observation of configurations in Section 2 and methods in
480 Section 3.

481 Guidelines:

- 482 • The answer NA means that the abstract and introduction do not include the claims
483 made in the paper.
- 484 • The abstract and/or introduction should clearly state the claims made, including the
485 contributions made in the paper and important assumptions and limitations. A No or
486 NA answer to this question will not be perceived well by the reviewers.
- 487 • The claims made should match theoretical and experimental results, and reflect how
488 much the results can be expected to generalize to other settings.
- 489 • It is fine to include aspirational goals as motivation as long as it is clear that these goals
490 are not attained by the paper.

491 **2. Limitations**

492 Question: Does the paper discuss the limitations of the work performed by the authors?

493 Answer: [Yes]

494 Justification: We discuss present limitations and future plans in Section 5.

495 Guidelines:

- 496 • The answer NA means that the paper has no limitation while the answer No means that
497 the paper has limitations, but those are not discussed in the paper.
- 498 • The authors are encouraged to create a separate "Limitations" section in their paper.
- 499 • The paper should point out any strong assumptions and how robust the results are to
500 violations of these assumptions (e.g., independence assumptions, noiseless settings,
501 model well-specification, asymptotic approximations only holding locally). The authors
502 should reflect on how these assumptions might be violated in practice and what the
503 implications would be.
- 504 • The authors should reflect on the scope of the claims made, e.g., if the approach was
505 only tested on a few datasets or with a few runs. In general, empirical results often
506 depend on implicit assumptions, which should be articulated.
- 507 • The authors should reflect on the factors that influence the performance of the approach.
508 For example, a facial recognition algorithm may perform poorly when image resolution
509 is low or images are taken in low lighting. Or a speech-to-text system might not be
510 used reliably to provide closed captions for online lectures because it fails to handle
511 technical jargon.
- 512 • The authors should discuss the computational efficiency of the proposed algorithms
513 and how they scale with dataset size.
- 514 • If applicable, the authors should discuss possible limitations of their approach to
515 address problems of privacy and fairness.
- 516 • While the authors might fear that complete honesty about limitations might be used by
517 reviewers as grounds for rejection, a worse outcome might be that reviewers discover
518 limitations that aren't acknowledged in the paper. The authors should use their best
519 judgment and recognize that individual actions in favor of transparency play an impor-
520 tant role in developing norms that preserve the integrity of the community. Reviewers
521 will be specifically instructed to not penalize honesty concerning limitations.

522 **3. Theory assumptions and proofs**

523 Question: For each theoretical result, does the paper provide the full set of assumptions and
524 a complete (and correct) proof?

525 Answer: [NA]

526 Justification: Our research presents a practical approach to mixing configurations for down-
527 stream predictions. No novel theoretical claims are made that require formal proof.

528 Guidelines:

- 529 • The answer NA means that the paper does not include theoretical results.
- 530 • All the theorems, formulas, and proofs in the paper should be numbered and cross-
531 referenced.
- 532 • All assumptions should be clearly stated or referenced in the statement of any theorems.
- 533 • The proofs can either appear in the main paper or the supplemental material, but if
534 they appear in the supplemental material, the authors are encouraged to provide a short
535 proof sketch to provide intuition.
- 536 • Inversely, any informal proof provided in the core of the paper should be complemented
537 by formal proofs provided in appendix or supplemental material.
- 538 • Theorems and Lemmas that the proof relies upon should be properly referenced.

539 4. Experimental result reproducibility

540 Question: Does the paper fully disclose all the information needed to reproduce the main ex-
541 perimental results of the paper to the extent that it affects the main claims and/or conclusions
542 of the paper (regardless of whether the code and data are provided or not)?

543 Answer: [Yes]

544 Justification: To ensure complete reproducibility, we provide all necessary information
545 in Section 3, Section 4 and Appendix. It includes methodologies, experiment setups,
546 computing environment, parameter settings and other implementation details, enabling
547 independent verification of all our claims and conclusions.

548 Guidelines:

- 549 • The answer NA means that the paper does not include experiments.
- 550 • If the paper includes experiments, a No answer to this question will not be perceived
551 well by the reviewers: Making the paper reproducible is important, regardless of
552 whether the code and data are provided or not.
- 553 • If the contribution is a dataset and/or model, the authors should describe the steps taken
554 to make their results reproducible or verifiable.
- 555 • Depending on the contribution, reproducibility can be accomplished in various ways.
556 For example, if the contribution is a novel architecture, describing the architecture fully
557 might suffice, or if the contribution is a specific model and empirical evaluation, it may
558 be necessary to either make it possible for others to replicate the model with the same
559 dataset, or provide access to the model. In general, releasing code and data is often
560 one good way to accomplish this, but reproducibility can also be provided via detailed
561 instructions for how to replicate the results, access to a hosted model (e.g., in the case
562 of a large language model), releasing of a model checkpoint, or other means that are
563 appropriate to the research performed.
- 564 • While NeurIPS does not require releasing code, the conference does require all submis-
565 sions to provide some reasonable avenue for reproducibility, which may depend on the
566 nature of the contribution. For example
 - 567 (a) If the contribution is primarily a new algorithm, the paper should make it clear how
568 to reproduce that algorithm.
 - 569 (b) If the contribution is primarily a new model architecture, the paper should describe
570 the architecture clearly and fully.
 - 571 (c) If the contribution is a new model (e.g., a large language model), then there should
572 either be a way to access this model for reproducing the results or a way to reproduce
573 the model (e.g., with an open-source dataset or instructions for how to construct
574 the dataset).
 - 575 (d) We recognize that reproducibility may be tricky in some cases, in which case
576 authors are welcome to describe the particular way they provide for reproducibility.
577 In the case of closed-source models, it may be that access to the model is limited in
578 some way (e.g., to registered users), but it should be possible for other researchers
579 to have some path to reproducing or verifying the results.

580 **5. Open access to data and code**

581 Question: Does the paper provide open access to the data and code, with sufficient instruc-
582 tions to faithfully reproduce the main experimental results, as described in supplemental
583 material?

584 Answer: [Yes]

585 Justification: We have made our code and data publicly accessible through the GitHub links
586 provided in this paper.

587 Guidelines:

- 588 • The answer NA means that paper does not include experiments requiring code.
- 589 • Please see the NeurIPS code and data submission guidelines (<https://nips.cc/public/guides/CodeSubmissionPolicy>) for more details.
- 590 • While we encourage the release of code and data, we understand that this might not be
591 possible, so “No” is an acceptable answer. Papers cannot be rejected simply for not
592 including code, unless this is central to the contribution (e.g., for a new open-source
593 benchmark).
- 594 • The instructions should contain the exact command and environment needed to run to
595 reproduce the results. See the NeurIPS code and data submission guidelines (<https://nips.cc/public/guides/CodeSubmissionPolicy>) for more details.
- 596 • The authors should provide instructions on data access and preparation, including how
597 to access the raw data, preprocessed data, intermediate data, and generated data, etc.
- 598 • The authors should provide scripts to reproduce all experimental results for the new
599 proposed method and baselines. If only a subset of experiments are reproducible, they
600 should state which ones are omitted from the script and why.
- 601 • At submission time, to preserve anonymity, the authors should release anonymized
602 versions (if applicable).
- 603 • Providing as much information as possible in supplemental material (appended to the
604 paper) is recommended, but including URLs to data and code is permitted.

607 **6. Experimental setting/details**

608 Question: Does the paper specify all the training and test details (e.g., data splits, hyper-
609 parameters, how they were chosen, type of optimizer, etc.) necessary to understand the
610 results?

611 Answer: [Yes]

612 Justification: We specify all the Implementation details and experimental setup in Sec-
613 tion 4.1.

614 Guidelines:

- 615 • The answer NA means that the paper does not include experiments.
- 616 • The experimental setting should be presented in the core of the paper to a level of detail
617 that is necessary to appreciate the results and make sense of them.
- 618 • The full details can be provided either with the code, in appendix, or as supplemental
619 material.

620 **7. Experiment statistical significance**

621 Question: Does the paper report error bars suitably and correctly defined or other appropriate
622 information about the statistical significance of the experiments?

623 Answer: [Yes]

624 Justification: The paper includes error bars for key results (e.g., Table 1), clearly stating they
625 represent standard deviation over multiple runs with different seeds.

626 Guidelines:

- 627 • The answer NA means that the paper does not include experiments.
- 628 • The authors should answer "Yes" if the results are accompanied by error bars, confi-
629 dence intervals, or statistical significance tests, at least for the experiments that support
630 the main claims of the paper.

- 631 • The factors of variability that the error bars are capturing should be clearly stated (for
 632 example, train/test split, initialization, random drawing of some parameter, or overall
 633 run with given experimental conditions).
 634 • The method for calculating the error bars should be explained (closed form formula,
 635 call to a library function, bootstrap, etc.)
 636 • The assumptions made should be given (e.g., Normally distributed errors).
 637 • It should be clear whether the error bar is the standard deviation or the standard error
 638 of the mean.
 639 • It is OK to report 1-sigma error bars, but one should state it. The authors should
 640 preferably report a 2-sigma error bar than state that they have a 96% CI, if the hypothesis
 641 of Normality of errors is not verified.
 642 • For asymmetric distributions, the authors should be careful not to show in tables or
 643 figures symmetric error bars that would yield results that are out of range (e.g. negative
 644 error rates).
 645 • If error bars are reported in tables or plots, The authors should explain in the text how
 646 they were calculated and reference the corresponding figures or tables in the text.

647 **8. Experiments compute resources**

648 Question: For each experiment, does the paper provide sufficient information on the com-
 649 puter resources (type of compute workers, memory, time of execution) needed to reproduce
 650 the experiments?

651 Answer: [Yes]

652 Justification: We detail the experimental environment in Section 4.1 and compare the time
 653 of execution between different clustering methods in Fig. 10.

654 Guidelines:

- 655 • The answer NA means that the paper does not include experiments.
 656 • The paper should indicate the type of compute workers CPU or GPU, internal cluster,
 657 or cloud provider, including relevant memory and storage.
 658 • The paper should provide the amount of compute required for each of the individual
 659 experimental runs as well as estimate the total compute.
 660 • The paper should disclose whether the full research project required more compute
 661 than the experiments reported in the paper (e.g., preliminary or failed experiments that
 662 didn't make it into the paper).

663 **9. Code of ethics**

664 Question: Does the research conducted in the paper conform, in every respect, with the
 665 NeurIPS Code of Ethics <https://neurips.cc/public/EthicsGuidelines>?

666 Answer: [Yes]

667 Justification: Our research conforms with every aspect of the NeurIPS Code of Ethics.

668 Guidelines:

- 669 • The answer NA means that the authors have not reviewed the NeurIPS Code of Ethics.
 670 • If the authors answer No, they should explain the special circumstances that require a
 671 deviation from the Code of Ethics.
 672 • The authors should make sure to preserve anonymity (e.g., if there is a special consid-
 673 eration due to laws or regulations in their jurisdiction).

674 **10. Broader impacts**

675 Question: Does the paper discuss both potential positive societal impacts and negative
 676 societal impacts of the work performed?

677 Answer: [NA]

678 Justification: Our research primarily contributes to improving technical aspects of down-
 679 stream prediction tasks and does not have broader societal implications.

680 Guidelines:

- 681 • The answer NA means that there is no societal impact of the work performed.

- 682 • If the authors answer NA or No, they should explain why their work has no societal
683 impact or why the paper does not address societal impact.
- 684 • Examples of negative societal impacts include potential malicious or unintended uses
685 (e.g., disinformation, generating fake profiles, surveillance), fairness considerations
686 (e.g., deployment of technologies that could make decisions that unfairly impact specific
687 groups), privacy considerations, and security considerations.
- 688 • The conference expects that many papers will be foundational research and not tied
689 to particular applications, let alone deployments. However, if there is a direct path to
690 any negative applications, the authors should point it out. For example, it is legitimate
691 to point out that an improvement in the quality of generative models could be used to
692 generate deepfakes for disinformation. On the other hand, it is not needed to point out
693 that a generic algorithm for optimizing neural networks could enable people to train
694 models that generate Deepfakes faster.
- 695 • The authors should consider possible harms that could arise when the technology is
696 being used as intended and functioning correctly, harms that could arise when the
697 technology is being used as intended but gives incorrect results, and harms following
698 from (intentional or unintentional) misuse of the technology.
- 699 • If there are negative societal impacts, the authors could also discuss possible mitigation
700 strategies (e.g., gated release of models, providing defenses in addition to attacks,
701 mechanisms for monitoring misuse, mechanisms to monitor how a system learns from
702 feedback over time, improving the efficiency and accessibility of ML).

703 11. Safeguards

704 Question: Does the paper describe safeguards that have been put in place for responsible
705 release of data or models that have a high risk for misuse (e.g., pretrained language models,
706 image generators, or scraped datasets)?

707 Answer: [NA]

708 Justification: The models and data presented in our work do not pose any risks of misuse.

709 Guidelines:

- 710 • The answer NA means that the paper poses no such risks.
- 711 • Released models that have a high risk for misuse or dual-use should be released with
712 necessary safeguards to allow for controlled use of the model, for example by requiring
713 that users adhere to usage guidelines or restrictions to access the model or implementing
714 safety filters.
- 715 • Datasets that have been scraped from the Internet could pose safety risks. The authors
716 should describe how they avoided releasing unsafe images.
- 717 • We recognize that providing effective safeguards is challenging, and many papers do
718 not require this, but we encourage authors to take this into account and make a best
719 faith effort.

720 12. Licenses for existing assets

721 Question: Are the creators or original owners of assets (e.g., code, data, models), used in
722 the paper, properly credited and are the license and terms of use explicitly mentioned and
723 properly respected?

724 Answer: [Yes]

725 Justification: For every dataset used in our research, we cite its original papers or official
726 websites. We properly credit all open-source packages used (e.g. pytorch).

727 Guidelines:

- 728 • The answer NA means that the paper does not use existing assets.
- 729 • The authors should cite the original paper that produced the code package or dataset.
- 730 • The authors should state which version of the asset is used and, if possible, include a
731 URL.
- 732 • The name of the license (e.g., CC-BY 4.0) should be included for each asset.
- 733 • For scraped data from a particular source (e.g., website), the copyright and terms of
734 service of that source should be provided.

- 735 • If assets are released, the license, copyright information, and terms of use in the
736 package should be provided. For popular datasets, paperswithcode.com/datasets
737 has curated licenses for some datasets. Their licensing guide can help determine the
738 license of a dataset.
739 • For existing datasets that are re-packaged, both the original license and the license of
740 the derived asset (if it has changed) should be provided.
741 • If this information is not available online, the authors are encouraged to reach out to
742 the asset's creators.

743 **13. New assets**

744 Question: Are new assets introduced in the paper well documented and is the documentation
745 provided alongside the assets?

746 Answer: [Yes]

747 Justification: We have included README files in our released code repositories to provide
748 clear and comprehensive documentation.

749 Guidelines:

- 750 • The answer NA means that the paper does not release new assets.
751 • Researchers should communicate the details of the dataset/code/model as part of their
752 submissions via structured templates. This includes details about training, license,
753 limitations, etc.
754 • The paper should discuss whether and how consent was obtained from people whose
755 asset is used.
756 • At submission time, remember to anonymize your assets (if applicable). You can either
757 create an anonymized URL or include an anonymized zip file.

758 **14. Crowdsourcing and research with human subjects**

759 Question: For crowdsourcing experiments and research with human subjects, does the paper
760 include the full text of instructions given to participants and screenshots, if applicable, as
761 well as details about compensation (if any)?

762 Answer: [NA]

763 Justification: Our work does not involve crowdsourcing or research with human subjects.

764 Guidelines:

- 765 • The answer NA means that the paper does not involve crowdsourcing nor research with
766 human subjects.
767 • Including this information in the supplemental material is fine, but if the main contribu-
768 tion of the paper involves human subjects, then as much detail as possible should be
769 included in the main paper.
770 • According to the NeurIPS Code of Ethics, workers involved in data collection, curation,
771 or other labor should be paid at least the minimum wage in the country of the data
772 collector.

773 **15. Institutional review board (IRB) approvals or equivalent for research with human
774 subjects**

775 Question: Does the paper describe potential risks incurred by study participants, whether
776 such risks were disclosed to the subjects, and whether Institutional Review Board (IRB)
777 approvals (or an equivalent approval/review based on the requirements of your country or
778 institution) were obtained?

779 Answer: [NA]

780 Justification: Our work does not involve human experiments or study participants.

781 Guidelines:

- 782 • The answer NA means that the paper does not involve crowdsourcing nor research with
783 human subjects.
784 • Depending on the country in which research is conducted, IRB approval (or equivalent)
785 may be required for any human subjects research. If you obtained IRB approval, you
786 should clearly state this in the paper.

- 787 • We recognize that the procedures for this may vary significantly between institutions
788 and locations, and we expect authors to adhere to the NeurIPS Code of Ethics and the
789 guidelines for their institution.
790 • For initial submissions, do not include any information that would break anonymity (if
791 applicable), such as the institution conducting the review.

792 **16. Declaration of LLM usage**

793 Question: Does the paper describe the usage of LLMs if it is an important, original, or
794 non-standard component of the core methods in this research? Note that if the LLM is used
795 only for writing, editing, or formatting purposes and does not impact the core methodology,
796 scientific rigorousness, or originality of the research, declaration is not required.

797 Answer: [NA]

798 Justification: LLMs are not involved in core method development of our research.

799 Guidelines:

- 800 • The answer NA means that the core method development in this research does not
801 involve LLMs as any important, original, or non-standard components.
802 • Please refer to our LLM policy (<https://neurips.cc/Conferences/2025/LLM>)
803 for what should or should not be described.